

Grain-boundary capacitance of $\text{La}_{0.7}\text{Ca}_{0.3}\text{MnO}_3$ films

A. Glaser and M. Ziese*

Department of Superconductivity and Magnetism, University of Leipzig, D-04103 Leipzig, Germany
(Received 22 February 2002; revised manuscript received 15 May 2002; published 18 September 2002)

The capacitance of grain boundaries formed at step edges in $\text{La}_{0.7}\text{Ca}_{0.3}\text{MnO}_3$ films was measured using impedance spectroscopy. The grain-boundary capacitance decreases with temperature and vanishes in the paramagnetic phase. The grain-boundary region is modeled as an abrupt metal-semiconductor contact inducing a depletion layer; the built in voltage is expected to be caused by chemical potential shifts due to differences in the ferromagnetic order in the grains and the grain boundaries. This model indicates that the capacitance vanishes with the second power of the difference between grain and grain-boundary magnetization; the data indicate that the capacitance follows more closely the grain-boundary magnetization as determined from the magnetoresistance.

DOI: 10.1103/PhysRevB.66.094422

PACS number(s): 75.30.Vn, 73.30.+y, 72.25.Mk

The magnetotransport properties of grain boundaries in colossal magnetoresistance (CMR) manganites have been under intense study in recent years.¹ This interest arose from the observation of a large low-field magnetoresistance in polycrystalline samples.² From magnetotransport, current-voltage, and local magnetic measurements the following picture for grain-boundary (GB) transport processes emerged: since the double exchange mechanism responsible for metallic conduction in the manganites depends sensitively on the Mn-O-Mn bond angle,³ structural disorder near the GB weakens double exchange and leads to a strong increase in resistivity. The GB region acts as a barrier for spin-polarized tunneling between adjacent grains; in weak magnetic fields the grains are aligned leading to the observed large resistance drop. The tunneling process is generally inelastic proceeding via few Mn ions localized in the barrier.^{4,5}

The microscopic nature of the GB region is not well understood so far. It has been assumed that the GB magnetization is suppressed compared to the bulk magnetization⁶ and magnetic force microscopy studies actually indicate differences between GB and grain magnetization; the Curie temperature near the GB, however, was found to be enhanced.⁷ Furukawa⁸ found a shift of the chemical potential $\Delta\mu$ as a function of the magnetization M in double exchange systems. Both, in the ferromagnetic and paramagnetic phase a scaling $\Delta\mu/W \propto M^2$ holds; W denotes the bandwidth and is estimated to $W=1$ eV.⁸ If this result is applied to a GB, there is a chemical potential shift between the GB region (with magnetization M_{gb}) and the grain (magnetization M_g) given by $\Delta\mu/W \propto (M_g^2 - M_{gb}^2)$. This might induce a depletion layer in the GB region; the corresponding space charges induce a capacitance. Here the GB capacitance of $\text{La}_{0.7}\text{Ca}_{0.3}\text{MnO}_3$ (LCMO) films as obtained from impedance spectroscopy is reported.

LCMO films were fabricated on virgin and patterned LaAlO_3 substrates by pulsed laser deposition from a stoichiometric polycrystalline target. Substrate temperature was 700 °C and oxygen partial pressure 100 mTorr. Substrate size is 5×5 mm². Step edges were fabricated on some of the substrates prior to deposition using conventional photolithography and subsequent chemically assisted ion-beam etching.⁹ Step heights were between 100 and 200 nm with

individual steps separated by a distance of 20 μm ; two sets of substrates with steps along [100] and [110] were studied. An atomic force microscopy (AFM) image of two step edges is shown in Fig. 1. In this work two LCMO films with step edges along [100] and [110] and a reference sample without step edges were investigated. Film thickness was estimated from deposition time to 20 nm ([100]), 25 nm ([110]), and 40 nm (epitaxial) with a typical error of 10%. The magnetization measured in an applied field of 0.1 T at 10 K was $\mu_0 M = 0.6$ T independent of film thickness within the error limits set by the thickness determination. The Curie temperatures of these films as determined from the inflection points in the magnetization versus temperature curves are 190 K ([100]), 216 K ([110]), and 230 K (epitaxial). The variation in the Curie temperatures is due to the different film thickness.^{10,11} The films containing step edges show a considerable low field magnetoresistance due to GBs formed at the step edges.⁹ The frequency dependent resistance of the samples was measured with a conventional four-probe technique with in-line silver-paste contacts. There were ten step edges between the voltage probes. Two-phase Lock-In detection was employed at measuring currents of 3 μA with frequencies in the range from 5 to 100 kHz. In order to eliminate phase errors induced by the setup only amplitude data will be discussed here. Magnetization measurements were performed in a SQUID magnetometer.

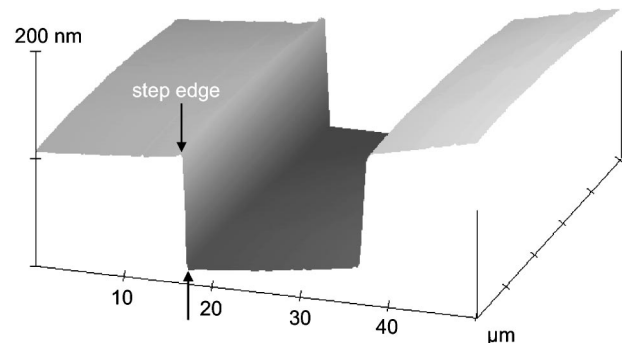


FIG. 1. AFM image of two step edges on a LaAlO_3 substrate. Grain boundaries might nucleate near the edges, such that there are two grain boundaries per step edge.

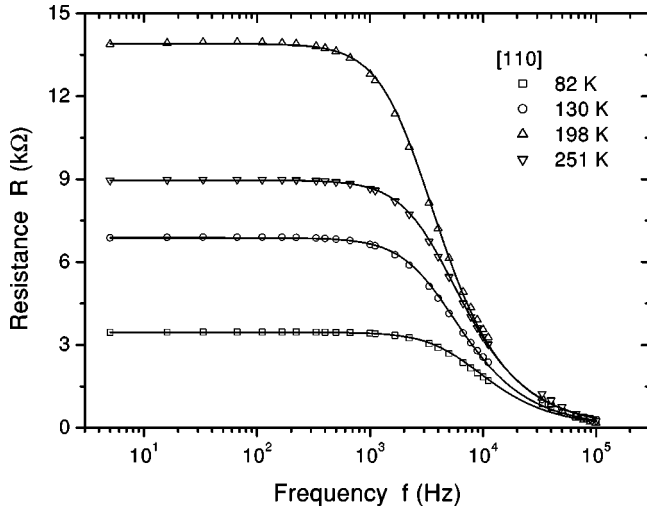


FIG. 2. Measured resistance amplitude of the LCMO film with [110] step edges as a function of frequency at various temperatures. The solid lines were obtained using equivalent circuit analysis.

Figure 2 shows raw amplitude data obtained on the LCMO sample with [110] step edges for various temperatures. The data show a strong decrease with frequency above about 1 kHz indicating capacitive effects. The capacitance arises from both sample and wiring. Since the grain resistance is much smaller than the GB resistance,² the measured frequency dependence is analyzed within an equivalent circuit as shown in Fig. 3. n denotes twice the number of step edges between the voltage contacts R_{gb} and C_{gb} , the GB resistance, and capacitance, respectively, and C_w the cable capacitance. The impedance of this circuit is given by

$$Z = \frac{nR_{gb}}{1 + i\omega nR_{gb}(C_{gb}/n + C_w)} \quad (1)$$

with the angular frequency $\omega = 2\pi f$. The cable capacitance $C_w = 2.8$ nF was determined by measurements of the frequency response of ohmic standard resistors and was subtracted from the data. The modulus of Eq. (1) was used to fit the data obtained on the LCMO samples; the fitted curves as shown in Fig. 2 agree well with the experimental data. Measurements as a function of frequency in the range $5 \text{ Hz} \leq f \leq 100 \text{ kHz}$ were performed every 5 K between 80 and 300 K. Each dataset was analyzed using Eq. (1) and the resulting

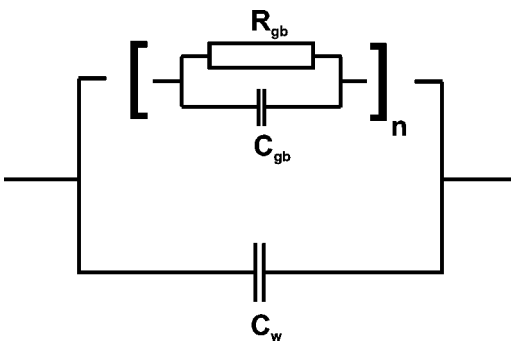


FIG. 3. Equivalent circuit used for the analysis of the impedance data.

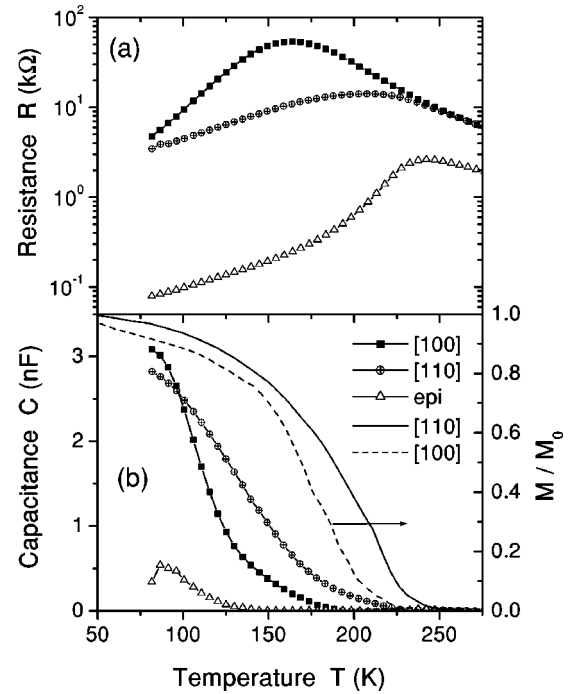


FIG. 4. (a) Resistance and (b) capacitance of the LCMO samples studied. The wire capacitance of 2.8 nF was subtracted. For the step edges nR_{gb} and C_{gb}/n are shown, whereas the total measured resistance and capacitance of the epitaxial film are presented. In (b) the normalized magnetization as measured in a SQUID magnetometer in a field of 100 mT is shown for the step-edge samples (right scale, solid line [110], dashed line [100]). M_0 denotes the magnetization at 0 K.

values of the GB resistance and capacitance are shown in Fig. 4. There are several features in these data to be noticed. (1) the GB resistance is indeed considerably higher than the resistance of the epitaxial film, especially in the low temperature regime. (2) The capacitance measured over the step edges decreases with temperature. The comparison with the reduced magnetization shows that the capacitance vanishes below the Curie temperature as defined by the vanishing of the magnetization. However, there is a slight difference in the Curie temperatures of the two step-edge samples which is manifested in both magnetization and capacitance curves. This indicates the relation of the capacitance to ferromagnetic order. (3) An additional capacitance is also measured for the epitaxial film at low temperatures. Since the capacitance measured over the step edges is clearly larger than this spurious capacitance, one might conclude that the former is induced by grain boundaries. With the film cross-section $A = 5 \text{ mm} \times d$, d being the film thickness, and the number of GBs $n \approx 20$ between the voltage contacts, at 100 K a typical areal GB resistance $R_{gb}A \approx 5 \times 10^{-4} \Omega \text{ cm}^2$ and a capacitance per area $C_{gb}/A \approx 2.5 \times 10^7 \text{ nF/cm}^2$ are obtained. These estimates are lower and upper bounds, respectively, since not every step edge must act as a high resistance GB (Ref. 12) and since the effective area might be increased due to interfacial roughness. The areal resistance obtained here is well in the range of previously reported values.^{2,5} The RC time constant is $\tau \approx 10 \mu\text{s}$. This is large compared to the crossover

frequency of about 80 MHz estimated by Yates *et al.* from an analysis of transport data on $\text{La}_{0.7-x}\text{Y}_x\text{Ca}_{0.3}\text{MnO}_3$ polycrystals.¹³ There are no capacitance data for CMR manganites available in the literature. The capacitance of semiconducting BaTiO_3 showing the positive temperature coefficient of resistance (PTCR) effect has been extensively measured; here typical values of 300 nF/cm^2 were found,^{14,15} much smaller than the capacitance values obtained here.

The data will be analyzed in a simplified model for the GB capacitance of a depletion layer. The GB region is modeled as a semiconductor adjacent to the metallic grain with a sharp interface. The built-in voltage V_{bi} is given by the chemical potential shift as discussed above: $V_{bi} = \Delta\mu \propto W(M_g^2 - M_{gb}^2)$. This shift can be as large as 0.1 W .⁸ If $V_{bi} \gg V_T$, the capacitance per area of the depletion layer is given by¹⁶

$$C = \sqrt{\frac{\epsilon_r \epsilon_0 e N_D}{2 V_{bi}}}, \quad (2)$$

with the vacuum permittivity ϵ_0 , relative permittivity ϵ_r , and donor density N_D . In case of nondegenerate semiconductors V_T is given by $k_B T/e$, whereas in case of a degenerate semiconductor one has $V_T = 1/[e \partial \ln(n)/\partial \mu]$. Assuming $\epsilon_r \sim 100$, $N_D \sim 5 \times 10^{27} \text{ m}^{-3}$,¹⁷ $V_{bi} \sim 0.05 \text{ eV}$,⁸ one obtains a capacitance $C \sim 3 \times 10^5 \text{ nF/cm}^2$. This value is in between the values obtained for the manganites and those for BaTiO_3 .

Equation (2) is valid at low temperatures where $V_{bi} \gg V_T$; for a vanishing V_{bi} it is clearly unphysical, since in this case the capacitance has to vanish. The divergence in Eq. (2) stems from the fact that in the derivation the carrier density $n(x) = N_D \exp[eV(x)/kT]$ was assumed to be small compared to N_D and has been neglected. $V(x)$ denotes the potential distribution in the semiconductor and is taken to be negative. Here the depletion-layer capacitance will be derived without the assumption $|V(x)| \gg kT$. Figure 5 shows the geometry of the metal-semiconductor contact considered here. Near the interface a depletion layer with free carrier density $n(x) = N_D \exp[V(x)/V_T]$ is formed. The potential $V(x)$ is obtained from Poisson's equation with a charge density $\rho(x) = e[N_D - n(x)]$. Boundary conditions are $V(x) \rightarrow 0$ and $dV(x)/dx \rightarrow 0$ for $x \rightarrow \infty$ as well as $V(0) = -V_{bi}$. The charge per area in the depletion layer is given by

$$\begin{aligned} Q &= \epsilon_r \epsilon_0 \frac{dV}{dx}(x=0) \\ &= \sqrt{2 \epsilon_r \epsilon_0 e N_D V_{bi}} \left[1 - \frac{V_T}{V_{bi}} [1 - \exp(-V_{bi}/V_T)] \right]^{1/2}. \end{aligned} \quad (3)$$

In the following the carrier density in the depletion layer is approximated by a constant $n = N_D \exp(-V_{bi}/V_T)$. Then the thickness l_D of the depletion layer can be defined by $e(N_D - n)l_D = Q$. In the limit $V_{bi} \rightarrow 0$ this approaches the constant value $l_D = \sqrt{\epsilon_r \epsilon_0 V_T / e N_D}$. The capacitance per area is given by $C = dQ/dV_a$, where V_a is the applied voltage. This voltage induces an additional voltage V_x across the depletion layer such that the capacitance can be calculated from Eq. (3)

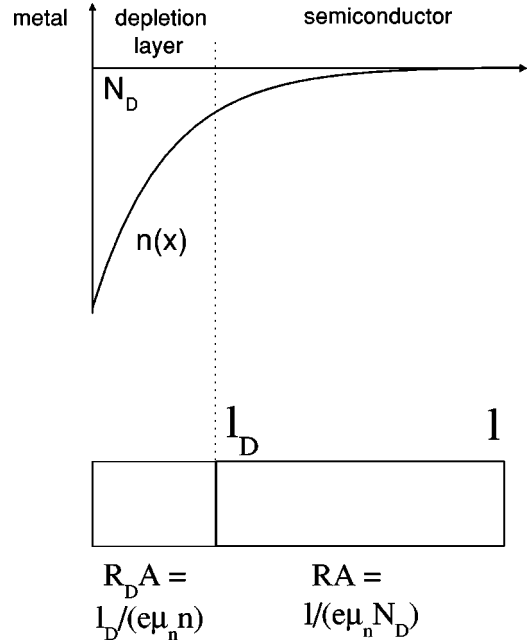


FIG. 5. Schematic drawing of the metal-semiconductor contact indicating the variation of the carrier density $n(x)$ and the thicknesses l_D of the depletion region and l of the bulklike semiconductor. At the bottom an equivalent circuit neglecting the resistance of the metal is indicated.

with the replacement $V_{bi} \rightarrow V_{bi} + V_x$. In the limit $n \ll N_D$ usually considered, the voltage drop occurs mainly over the depletion layer and $V_x \simeq V_a$. In the present case, however, the additional voltage appearing across the depletion layer vanishes in the limit $V_{bi} \rightarrow 0$ and V_x has to be calculated taking the ohmic resistances into account. If the resistances of the metal electrode and the bulk semiconductor are neglected, the excess voltage V_x is proportional to the difference of depletion layer conductivities for $V_{bi} > 0$ and $V_{bi} = 0$:

$$V_x = \frac{N_D - n}{N_D} V_a. \quad (4)$$

In the limit $V_{bi} \rightarrow 0$, one obtains for the capacitance $C = (\partial Q / \partial V_{bi})(\partial V_x / \partial V_a)$

$$C \simeq \frac{\epsilon_r \epsilon_0}{l_D} \frac{V_{bi}}{V_T}. \quad (5)$$

Since it is expected that

$$V_{bi} \propto (M_g^2 - M_{GB}^2), \quad (6)$$

the measured capacitance should be related to the difference of the second power of grain and GB magnetization. The grain magnetization M_g should be identical to the global magnetization as measured by the SQUID, since the volume fraction occupied by the GB's is vanishingly small. The GB magnetization is difficult to measure directly. On general grounds its magnitude is expected to be reduced compared to the grain magnetization; magnetic force microscopy indicates that the Curie temperature at the grain boundary might

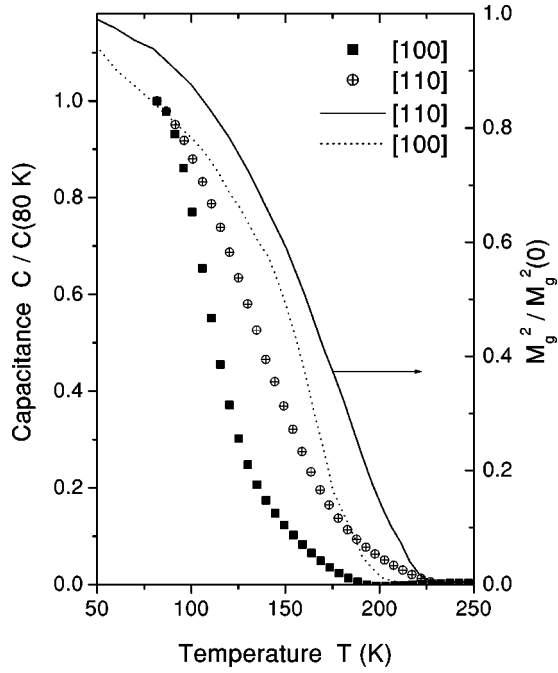


FIG. 6. Capacitance normalized by the value at 80 K of the step-edge samples (left axis) compared to the second power of the normalized grain magnetization (right axis).

not be reduced.⁷ Here we proceed as follows. First, in Fig. 6 the capacitance measured over the step edges is compared to the second power of the measured magnetization, thus entirely neglecting the GB contribution. For both samples the squared grain magnetization rises with decreasing temperature much steeper than the capacitance. This indicates that (a) there is a substantial GB magnetization M_{GB} or (b) Eq. (6) does not hold. As a second step we estimate the GB magnetization within the model of Evetts *et al.*:⁶ assuming a reduced GB magnetization these authors derived the low field magnetoresistance (MR) as

$$MR \propto M_{GB}^2 / M_g^2. \quad (7)$$

Using this equation the temperature dependence, but not the absolute magnitude, of the GB magnetization can be determined as $M_{GB} \propto M_g \sqrt{MR}$. The low field magnetoresistance was determined by the standard procedure,¹⁸ i.e., by establishing a reference resistance R_0 at zero field by linear extrapolation of the high field magnetoresistance and by defin-

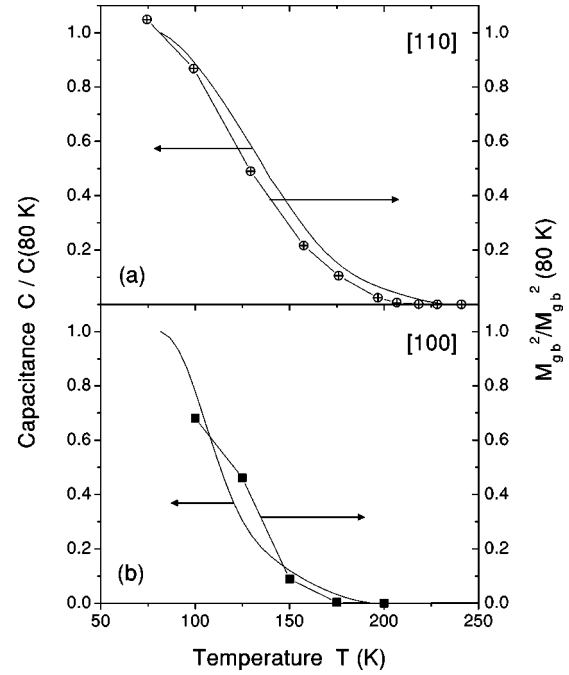


FIG. 7. Capacitance normalized by the value at 80 K of the step-edge samples (left axis) compared to the second power of the normalized grain-boundary magnetization (right axis). The GB magnetization was determined from the low field magnetoresistance.

ing $MR = [R(H_c) - R_0] / R_0$. H_c denotes the coercive field. Figure 7 shows the measured GB capacitance compared to the square of the GB magnetization; for the sample with [110] step edges the agreement is remarkably good, for the other sample it is reasonable. From these data we arrive at the conclusion that $C \propto M_{GB}^2$ in contrast to Eq. (6). However, one has to bear in mind that (a) this final result is highly model dependent and (b) Eq. (6) is based on theoretical calculations for the undistorted cubic phase. It is clearly desirable to develop a more detailed microscopic model of a GB in the manganites in order to understand the magnetotransport properties.

We thank Dr. R. Höhne, University of Leipzig, for general support, Dr. G. Heydon, University of Sheffield, for the AFM imaging, and J. Dienelt, Institute for Surface Modification, Leipzig, for the patterning of the substrates. This work was supported by the DFG under Contract No. DFG ES 86/7-1 within the Forschergruppe "Oxidische Grenzflächen."

*Electronic address: ziese@physik.uni-leipzig.de

¹M. Ziese, Rep. Prog. Phys. **65**, 143 (2002).

²A. Gupta, G.Q. Gong, G. Xiao, P.R. Duncombe, P. Lecoeur, P. Trouilloud, Y.Y. Wang, V.P. Dravid, and J.Z. Sun, Phys. Rev. B **54**, R15 629 (1996).

³J. Fontcuberta, B. Martínez, A. Seffar, S. Piñol, J.L. García-Muñoz, and X. Obradors, Phys. Rev. Lett. **76**, 1122 (1996).

⁴M. Ziese, Phys. Rev. B **60**, R738 (1999).

⁵J. Klein, C. Höfener, S. Uhlenbruck, L. Alff, B. Büchner, and R. Gross, Europhys. Lett. **47**, 371 (1999).

⁶J.E. Evetts, M.G. Blamire, N.D. Mathur, S.P. Isaac, B.-S. Teo,

L.F. Cohen, and J.L. MacManus-Driscoll, Philos. Trans. R. Soc. London, Ser. A **356**, 1593 (1998).

⁷Y.-A. Soh, G. Aeppli, N.D. Mathur, and M.G. Blamire, Phys. Rev. B **63**, 020402 (2001).

⁸N. Furukawa, J. Phys. Soc. Jpn. **66**, 2523 (1997).

⁹M. Ziese, G. Heydon, R. Höhne, P. Esquinazi, and J. Dienelt, Appl. Phys. Lett. **74**, 1481 (1999).

¹⁰T. Walter, K. Drr, K.-H. Müller, D. Eckert, K. Nenkov, M. Hecker, M. Lehmann, and L. Schultz, J. Magn. Magn. Mater. **222**, 175 (2000).

¹¹M. Ziese, H.C. Semmelhack, K.H. Han, S.P. Sena, and H. J.

- Blythe, J. Appl. Phys. (2002).
- ¹²X.L. Wang, S.X. Dou, H.K. Liu, M. Ionescu, and B. Zeimetz, Appl. Phys. Lett. **73**, 396 (1998).
- ¹³K.A. Yates, L.F. Cohen, C. Watine, T.-N. Tay, F. Damay, J. MacManus-Driscoll, R.S. Freitas, L. Ghivelder, E.M. Haines, and G.A. Gehring, J. Appl. Phys. **88**, 4703 (2000).
- ¹⁴P. Gerthsen and B. Hoffmann, Solid State Electron **16**, 617 (1973).
- ¹⁵D.C. Sinclair and A.R. West, J. Appl. Phys. **66**, 3850 (1989).
- ¹⁶W. Schottky, Z. Phys. **118**, 539 (1942).
- ¹⁷M. Ziese and C. Sritiwarawong, Europhys. Lett. **45**, 256 (1999).
- ¹⁸J.M.D. Coey, A.E. Berkowitz, L. Balcells, F.F. Putris, and A. Barry, Phys. Rev. Lett. **80**, 3815 (1998).